On the Bonding of First-Row Transition Metal Cations to Guanine and Adenine Nucleobases

M. Noguera, V. Branchadell, E. Constantino, R. Ríos-Font, M. Sodupe,* and L. Rodríguez-Santiago*

Departament de Química, Universitat Autònoma Barcelona, Bellaterra 08193, Spain

Received: May 18, 2007; In Final Form: July 11, 2007

The binding of first-row transition metal monocations (Sc^+-Cu^+) to N7 of guanine and N7 or N3 of adenine nucleobases has been analyzed using the hybrid B3LYP density functional theory (DFT) method. The nature of the bonding is mainly electrostatic, the electronic ground state being mainly determined by metal−ligand repulsion. M^+−guanine binding energies are 18−27 kcal/mol larger than those of M^+−adenine, the difference decreasing along the row. Decomposition analysis shows that differences between guanine and adenine mainly arise from Pauli repulsion and the deformation terms, which are larger for adenine. Metal cation affinity values at this level of calculation are in very good agreement with experimental data obtained by Rodgers et al. (*J. Am. Chem. Soc.* **2002**, *124*, 2678) for adenine nucleobases.

Introduction

DNA interacts with metals in two clearly distinguished manners.[1−4] The first one consists of having metal cations interacting with the DNA backbone's phosphate groups through nonspecific interactions. These interactions are electrostatic in nature and are mainly established with alkaline and alkaline-earth metals, which can be found in cell media (e.g., Na^+, K^+, and Ca^{2+} are responsible for osmotic equilibrium in cells). These cations become disposed around DNA following the external part of the double helix. Screening of phosphate groups' negative charge diminishes electrostatic repulsion between phosphate backbones and thus favors DNA stability. On the other hand, we can find metal cations directly interacting with nitrogenated bases in an inner-shell coordination manner or indirectly through water molecules. Metal cations that prefer this mode of interaction are usually found to be transition metals and the interaction is usually not solely electrostatic. Although the second type of interaction is quantitatively inferior, it may modify DNA in an irreversible way. One illustrative case for this kind of metal−DNA interaction is the cisplatin molecule, which links two consecutive bases together and is used as an anticarcinogenic drug. Cisplatin was discovered by Rosenberg[5] and has been one of the main subjects of investigation on the metal−DNA field because of its significance in the pharmacological world. Therefore, although cation−phosphate interactions are predominant, the binding of metal ions to the bases is not negligible, especially at high concentrations, and can modify the hydrogen bonding and the stacking interactions that stabilize the double helix.[3,4]

Because of the important role that metal cation−nucleobase interactions play in the stability of DNA, in the last 10 years, many efforts have been devoted, both experimentally[6−10] and theoretically,[10−31] to studying the fundamental nature of these interactions as well as to determine the metal cation affinity of nucleobases. In particular, threshold collision-induced dissociation experiments have been performed to determine bond dissociation energies of alkali metal cations to uracil, thymine, and adenine.[7] Alkali metal ion affinities to DNA nucleobases have also been determined by the modified approach of the kinetic method.[6]

The influence of d orbital occupation on the binding of first-row transition metal ions (Sc^+-Cu^+) to adenine has been analyzed by means of threshold collision induced dissociation methods in guided ion beam mass spectrometry experiments.[8] This study provides trends along the row, which can be rationalized by electronic structure calculations. Moreover, theoretical calculations can provide insights on the binding mechanisms that can help us understand more complex situations with different chemical environments.

Methods

The nonlocal hybrid three-parameter B3LYP[32−34] density functional has been used throughout the study because previous theoretical calculations have shown that B3LYP approach is a cost-effective method for studying transition metal ligand systems.[35−38] Even in difficult cases such as the $M^+{=}CH_2$ systems, B3LYP results compare well to the highly correlated CCSD(T) or multireference ACPF methods, as well as to the experimental values.[39]

Geometry optimizations and frequency calculations have been performed using a basis set that will be referred to as BSI. The metal basis is derived from the (14s9p5d) primitive set of Wachters[40] supplemented with one s, two p, one d diffuse functions, and one f polarization function, the final contracted basis set being [10s7p4d1f]. For C, N, O, and H, we have used the 6-31++G(d,p) basis set. Final binding energies, however, have been obtained from single-point calculations using a larger basis set. For the metal cation, the basis set is (15s11p6d3f1g)[10s7p4d3f1g] and for C, N, O, and H, we have used the 6-311++G(3df,2pd) one. This basis set will be denoted as BSII. Except for the Fe^+ complexes, binding energies have been computed with respect to the ground state of the metal cation, assuming adequate d occupations that correspond to a single determinantal representation of the desired atomic term.[38]

* Corresponding author. E-mail: luis@klingon.uab.es (L.R.S.); mariona@klingon.uab.es (M.S.).

10.1021/jp073858k CCC: $37.00
Published on Web 08/31/2007

SCHEME 1

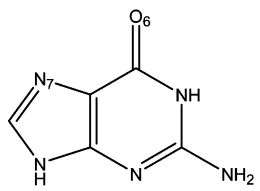

Guanine

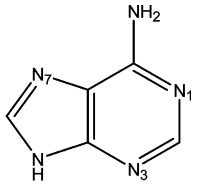

Adenine

For Fe^+, binding energies have been determined with respect to the Fe^+ ($3d^7$) asymptote, because this is the metal electronic configuration in the ground state M^+−adenine and M^+−guanine complexes, and we have then corrected the obtained interaction energy with the experimental energy difference between the $^6D(3d^64s^1)$ and the $^4F(3d^7)$ states (5.8 kcal/mol). Such a procedure has been used previously[35] and gives accurate results for binding energies in cases where DFT methods do not provide the correct atomic ground state.

Thermodynamic corrections have been obtained assuming an ideal gas, unscaled harmonic vibrational frequencies, and the rigid rotor approximation by standard statistical mechanical methods.[41] Net atomic charges and spin densities have been obtained using the natural population analysis of Weinhold et al.[42] Open shell calculations have been performed using an unrestricted formalism. For all those calculations the Gaussian 03 package has been employed.[43]

Additional single-point calculations have been carried out for Cu^+−guanine and Cu^+−adenine using the binding energy partition scheme implemented in the ADF program.[44,45] This scheme has been widely applied to a large number of systems including transition-metal-containing ones.[46,47] As hybrid functionals are not available in ADF, the analysis has been made using the BLYP functional at the geometries obtained with B3LYP. A triple-ζ plus polarization basis set has been used.

Results and Discussion

Metal ions can bind to different basic centers of purine nucleobases. For guanine, there is a general consensus that coordination to the N7 site is the preferred one. Additional stabilization is achieved in this position via the interaction with the O6 site, in such a way that calculations for bare metal cations interacting with guanine show a (N7, O6)-bidentate coordination mode.

For adenine, previous studies support that the preferred coordination is also bidentate involving the N7 and the N6 of the amino group, which rotates out of the plane and rehybridizes from sp^2 to sp^3 to optimize metal complexation (see Scheme 1). Nevertheless, previous studies have indicated that N3 coordination can be competitive.[8] Because of that, we have also investigated structures in which the metal cation is attached to the N3 of adenine.

Detailed Analysis of the Bonding. The binding between M^+ and guanine and adenine is mainly electrostatic, and because at a given bond length the electrostatic interaction is essentially independent of the orientation of the metal 3d and 4s electrons, the ordering of states is determined primarily by Pauli repulsion. Thus, the most important factor in determining the ground state is the minimization of the overlap between the metal 3d orbitals and the lone pairs of the ligand, guanine or adenine. Nevertheless, other factors such as 4s3d and 4p3d mixing or charge-transfer processes can also contribute to determine the ground state of M^+−guanine or M^+−adenine.

Isolated guanine and adenine have C_1 symmetry due to the fact that the amino group is not planar.[48,49] However, metal cation binding induces NH_2 planarity and thus M^+−guanine and M^+−adenine systems have C_s symmetry. As an example, and in order to aid in the discussion of the ground electronic state of M^+−guanine and M^+−adenine systems, the metal-cation-centered d orbitals for the case of Cu^+ are shown in Figure 1. By taking the molecular plane as *xz*, it can be observed that for Cu^+−guanine, the order of overlap is

$$3d_{z^2}(a') \approx 3d_{yz}(a'') < 3d_{xy}(a'') < 3d_{x^2-y^2}(a') \ll 3d_{xz}(a')$$

For Cu^+−adenine (N7,N6), both the d_{yz} and d_{xy} orbitals of the metal are mixed and the energy order of the first three orbitals is somewhat different from those found for guanine (N7, O6). In any case, both for Cu^+−guanine (N7, O6) and Cu^+−adenine (N7, N6), the $3d_{xz}$ orbital shows a much more important overlap with the purine than the other four orbitals because its lobules point directly toward the N and O lone pairs of the ligand, which results in a higher repulsion. The other four metal d orbitals show, in general, a small overlap with the orbitals of the ligand. For Cu^+−adenine (N3), the lobule of the d_{z^2} orbital points toward the lone pair of the N3 atom of the ligand. Thus, in this case, the d_{z^2} orbital is the one that shows the larger overlap with the base. The other four d metal orbitals show small overlap with the ligand, as in the previous cases.

We next consider the M^+−guanine and M^+−adenine bond for the metal cations Sc^+ to Cu^+. We have explored several electronic states in order to ensure that we have identified the ground state of each system. The results are summarized in Tables 1−3. For all M^+−adenine systems except Sc^+−adenine and Cr^+−adenine, the bidentate coordination through N7 and N6 is the preferred one. For Sc^+ and Cr^+, the metal cation prefers the N3 coordination. Thus, the following discussion always refers to the preferred coordination of each system.

For Sc^+ systems (Sc^+−guanine and Sc^+−adenine), the $^3A''$ ground state derives from the $3d^14s^1$ ground configuration of Sc^+, with the d electron primarily in the $3d_{yz}(a'')$ orbital for Sc^+−guanine (N7, O6) or in the $3d_{xy}(a'')$ orbital for Sc^+−adenine (N3). The natural 3d population (1.29 for guanine and 1.30 for adenine) indicates a significant contribution of the $3d^2$ configuration of Sc^+, as reflected also by the 4s3d hybridization (the natural population of the 4s orbital is 0.75 guanine and 0.83 for adenine). Such hybridization reduces the charge density between the metal cation and the lone pairs of the N and O atoms of the ligand, resulting in a smaller Pauli repulsion. The $^3A'$ state is very similar in energy to the ground state and derives from the $3d^14s^1$ configuration of Sc^+. However, now the d electron is in the $3d_{z^2}(a')$ orbital for Sc^+-guanine or in the $3d_{x^2-y^2}(a')$ orbital for Sc^+−adenine (N3). Similar to the ground state, there is an important contribution of the $3d^2$ configuration of the metal cation and the 4s3d is the mechanism used to reduce repulsion.

The ground state of Ti^+−guanine and Ti^+−adenine is a $^4A''$ state and arises from a $3d^24s^1$ configuration of Ti^+ with the two d electrons occupying the lowest 3d(a′) and 3d(a″) orbitals. The natural population of the 4s and 3d orbitals (about 0.6 and 2.5, respectively) indicates an important contribution of the $3d^3$ (^4F) asymptote. The mixing with this configuration and, consequently, the 4s3d hybridization to reduce repulsion is more important in this case than for Sc^+ because the $3d^{n+1}-3d^n4s^1$ separation is much smaller in Ti^+ than in Sc^+ (the experimental values are 2.46 and 13.73 kcal/mol respectively).[35] Furthermore, at the B3LYP level, the $3d^{n+1}$ configuration of Ti^+ becomes more stable than the $3d^n4s^1$ (the separation is −5.02 at the

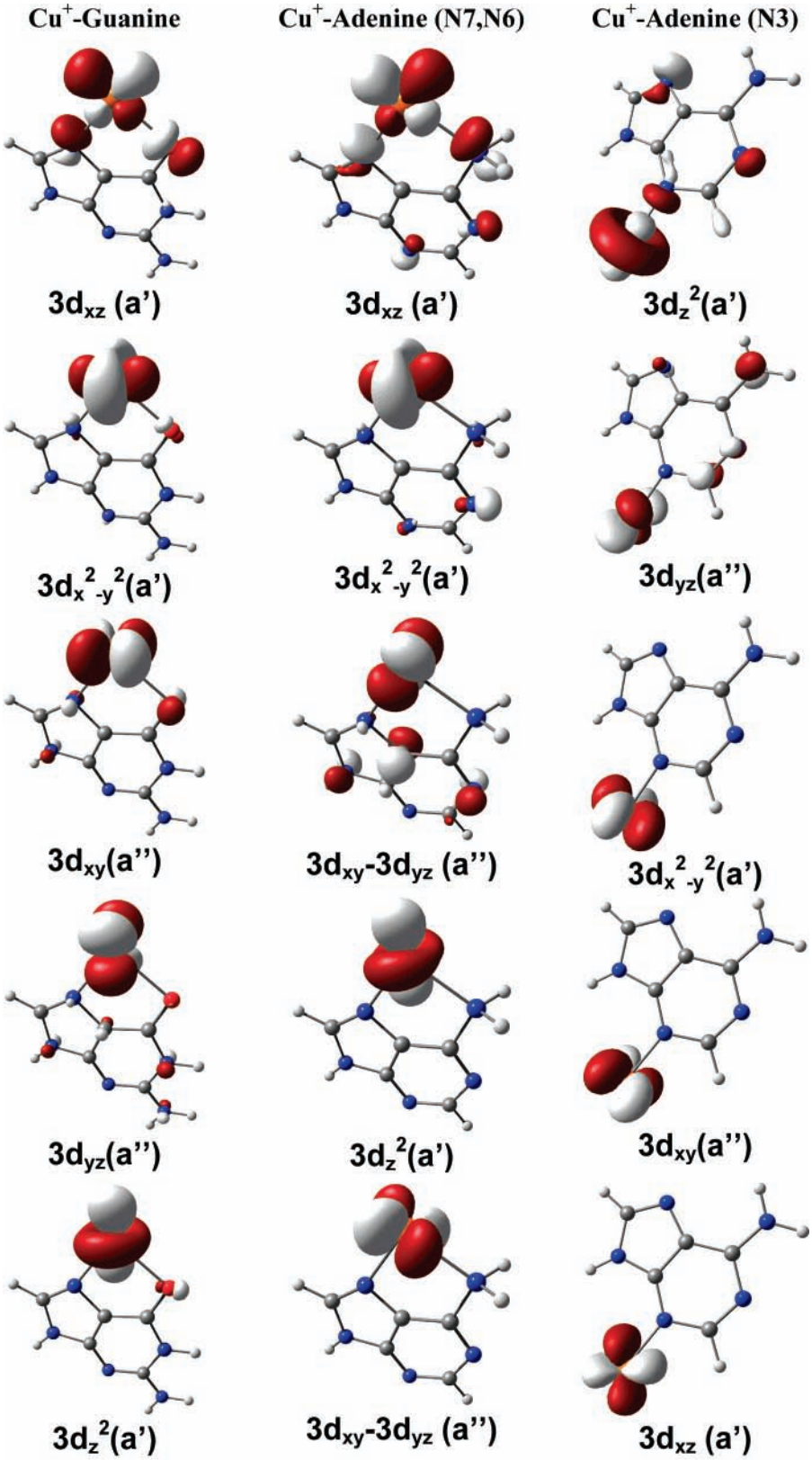

Figure 1. Metal-cation-centered d orbitals of N7,O6-coordinated Cu^+−guanine, N7,N6-coordinated Cu^+−adenine, and N3-coordinated Cu^+−adenine.

B3LYP level), denoting that the 4s to 3d promotion may be somewhat overestimated in this case. The $^4A'$ excited state of Ti^+−guanine and Ti^+−adenine is about 4−5 kcal/mol above the ground state. This state arises from the same configuration of Ti^+ ($3d^24s^1$) but now the occupied d orbitals are the two 3d(a″) ones. The 4s3d(a′) hybridization is similar to that found for the ground state, as illustrated by the 3d and 4s natural population.

The ground state of V^+−guanine and V^+−adenine is the $^5A'$ state. Once again, the natural population shows a large mixing of the 4s and 3d orbitals, even though the ground state of V^+ is $^5D(3d^4)$. This shows the efficiency of the 4s3d hybridization

TABLE 1: Binding Energies at the B3LYP/BSII Level (in kcal/mol), Metal Charge and Spin Density Values, and 3d, 4s, and 4p Metal Population for M^+−guanine Systems in the Considered Electronic State

M^+	electronic state	D_e	D_0[a]	ΔH^0_{298}	q_{M^+}	$spin_{M^+}$	3d	4s	4p
Sc^+	$^3A'$	77.7	76.7	77.0	0.868	1.968	1.39	0.71	0.01
Sc^+	$^3A''$	80.4	79.7	80.0	0.934	1.873	1.29	0.75	0.02
Ti^+	$^4A'$	82.1	81.1	81.4	0.873	2.926	2.52	0.58	0.02
Ti^+	$^4A''$	86.4	85.5	85.7	0.851	2.946	2.52	0.60	0.02
V^+	$^5A'$	87.2	86.1	86.4	0.829	3.959	3.72	0.43	0.01
Cr^+	$^6A'$	73.0	72.2	72.3	0.890	4.944	4.90	0.18	0.02
Mn^+	$^7A'$	71.1	70.2	70.3	0.873	5.862	5.05	1.01	0.05
Mn^+	$^5A'$	63.6	62.5	62.7	0.833	3.965	5.40	0.74	0.02
Mn^+	$^5A''$	55.6	55.0	55.2	0.962	4.046	5.86	0.14	0.02
Fe^+	$^4A'$	79.8	78.7	79.0	0.832	2.938	6.84	0.30	0.02
Fe^+	$^4A''$	79.5	78.5	78.8	0.856	2.955	6.86	0.25	0.02
Fe^+	$^6A'$	77.1	76.2	76.4	0.835	4.826	6.06	1.06	0.01
Fe^+	$^6A''$	77.9	76.9	77.2	0.839	4.828	6.08	1.02	0.01
Co^+	$^3A'$	88.7	87.7	87.9	0.861	1.961	7.99	0.13	0.02
Co^+	$^3A''$	88.0	86.9	87.2	0.846	1.954	7.94	0.19	0.02
Ni^+	$^2A'$	95.9	94.7	95.1	0.821	0.935	8.96	0.20	0.01
Ni^+	$^2A''$	85.0	84.0	84.2	0.863	0.993	8.93	0.18	0.02
Cu^+	$^1A'$	88.3	87.2	87.5	0.860		9.94	0.17	0.02

[a] Determined using the B3LYP/BSII D_e value and the B3LYP/BSI unscaled harmonic frequencies.

TABLE 2: Metal−Adenine Binding Energies at the B3LYP/BSII Level (in kcal/mol), Metal Charge and Spin Density Values, and 3d, 4s and 4p Metal Population for M^+−Adenine(N7,N6) Systems in the Considered Electronic State

M^+	electronic state	D_e	D_0[a]	ΔH^0_{298}	q_{M^+}	$spin_{M^+}$	3d	4s	4p
Sc^+	$^3A'$	53.7	52.7	53.7	0.879	1.963	1.39	0.71	0.01
Sc^+	$^3A''$	53.9	52.8	53.4	0.908	1.919	1.33	0.75	0.01
Ti^+	$^4A'$	58.6	57.3	58.0	0.881	2.930	2.59	0.51	0.01
Ti^+	$^4A''$	63.4	62.1	62.6	0.840	2.963	2.54	0.61	0.01
V^+	$^5A'$	65.6	64.1	64.8	0.819	3.969	3.75	0.43	0.01
Cr^+	$^6A'$	51.9	50.7	51.2	0.885	4.946	4.90	0.19	0.02
Mn^+	$^7A'$	47.7	46.5	47.0	0.872	5.852	5.05	1.03	0.04
Mn^+	$^5A'$	42.0	40.6	41.2	0.823	3.969	5.44	0.71	0.02
Mn^+	$^5A''$	34.0	32.9	33.5	0.927	4.046	5.89	0.16	0.01
Fe^+	$^4A'$	60.5	59.0	59.6	0.819	2.939	6.86	0.30	0.01
Fe^+	$^4A''$	60.1	58.5	59.2	0.833	2.951	6.88	0.26	0.01
Fe^+	$^6A'$	54.6	53.3	53.8	0.832	4.812	6.06	1.05	0.01
Fe^+	$^6A''$	55.5	54.2	54.7	0.834	4.811	6.08	1.03	0.02
Co^+	$^3A'$	70.6	69.0	69.7	0.843	1.955	7.99	0.15	0.01
Co^+	$^3A''$	69.5	67.8	68.5	0.818	1.943	7.94	0.22	0.01
Ni^+	$^2A'$	78.7	76.6	77.6	0.796	0.926	8.96	0.23	0.01
Ni^+	$^2A''$	65.6	64.6	65.2	0.857	0.999	8.93	0.19	0.02
Cu^+	$^1A'$	70.6	69.0	69.7	0.845		9.93	0.20	0.01

[a] Determined using the B3LYP/BSII D_e value and the B3LYP/BSI unscaled harmonic frequencies.

on the left-hand side of the row because of the similar spatial extent of the 3d and 4s orbitals at this side of the row. However, this hybridization is somewhat less important than for Ti^+ because of the larger $3d^{n+1}-3d^n4s^1$ separation (7.78 kcal/mol). The excited $^5A''$ state has not been taken into account because it would imply the occupation of the $3d_{xz}(a')$ orbital, leading to an important increase in the repulsion with the lone pairs of N and O.

The $^6A'$ ground state of Cr^+−guanine and Cr^+−adenine is derived from the $^6S(3d^5)$ asymptote of Cr^+. The natural 3d population of Cr^+ in Cr^+−guanine (4.90 electrons) indicates a small 4s3d hybridization in this case. The occupation of the $3d_{xz}(a')$ orbital in Cr^+−guanine considerably increases repulsion with the ligand, resulting in a larger metal−ligand distance and therefore a decrease in the binding energy compared to the previous metal cations. However, in Cr^+−adenine, where the preferred coordination is through N3, the increase in repulsion due to occupation of the $3d_z^2$ orbital can be efficiently reduced by 4s3d hybridization (the natural 3d population of Cr^+ in Cr^+−adenine (N3) is 4.76) as reflected in the decrease of the metal−ligand distance with respect to the same coordination of the previous metal cations (see below).

TABLE 3: Metal−Adenine Binding Energies at the B3LYP/BSII Level (in kcal/mol), Metal Charge and Spin Density Values, and 3d, 4s and 4p Metal Population for M^+−Adenine(N3) Systems in the Considered Electronic State

M^+	electronic state	D_e	D_0[a]	ΔH^0_{298}	q_{M^+}	$spin_{M^+}$	3d	4s	4p
Sc^+	$^3A'$	55.3	54.3	54.6	0.871	1.99	1.29	0.83	0.01
Sc^+	$^3A''$	55.4	54.4	54.7	0.872	1.99	1.30	0.83	0.01
Ti^+	$^4A'$	53.5	52.5	52.9	0.886	2.96	2.49	0.63	0.01
Ti^+	$^4A''$	57.1	56.1	56.4	0.845	2.99	2.43	0.73	0.01
V^+	$^5A'$	57.1	56.0	56.4	0.834	4.00	3.52	0.64	0.01
Cr^+	$^6A'$	53.9	52.8	53.2	0.848	4.99	4.76	0.39	0.01
Mn^+	$^7A'$	47.1	46.2	46.5	0.877	5.87	5.06	1.02	0.04
Mn^+	$^5A'$	43.0	41.9	42.3	0.808	3.98	5.31	0.87	0.01
Mn^+	$^5A''$	29.6	28.5	28.9	0.866	3.98	5.92	0.20	0.01
Fe^+	$^4A'$	56.9	55.7	56.1	0.778	2.95	6.65	0.55	0.01
Fe^+	$^4A''$	56.9	55.8	56.2	0.778	2.95	6.65	0.55	0.01
Fe^+	$^6A'$	52.0	50.9	51.2	0.823	4.77	6.11	1.02	0.04
Fe^+	$^6A''$	51.9	50.8	51.2	0.826	4.78	6.11	1.02	0.04
Co^+	$^3A'$	64.2	63.1	63.5	0.854	1.99	7.96	0.18	0.01
Co^+	$^3A''$	64.5	63.2	63.7	0.817	1.96	7.85	0.32	0.01
Ni^+	$^2A'$	66.7	65.5	65.9	0.821	0.99	8.81	0.36	0.01
Ni^+	$^2A''$	67.9	65.5	65.9	0.810	0.95	8.90	0.31	0.01
Cu^+	$^1A'$	68.4	67.2	67.6	0.838		9.90	0.26	0.01

[a] Determined using the B3LYP/BSII D_e value and the B3LYP/BSI unscaled harmonic frequencies.

The ground state of Mn^+−guanine and Mn^+−adenine is a $^7A'$ state derived from the ground state of Mn^+ ($^7S(3d^54s^1)$) and the natural 3d population of Mn^+ is 5.05 electrons. The 4p population is somewhat larger than for the preceding cases because 4s4p hybridization is the only mechanism to reduce repulsion in this case. However, the magnitude of this hybridization is very small, as demonstrated by the natural 4p population (0.05 electrons) due to the high energy of the corresponding asymptote. The occupation of both $3d_{xz}(a')$ and 4s orbitals increases repulsion, as shown by the decrease in the binding energy of the $^7A'$ state of Mn^+−guanine and Mn^+−adenine compared to the previous Cr^+ complexes. The $^5D(3d^6)$ excited state is 41.70 kcal/mol higher in energy than the ground state[35] and thus the states of Mn^+−guanine and Mn^+−adenine derived from this configuration ($^5A'$ and $^5A''$) are higher in energy than the $^7A'$ state. In the $^5A'$ excited state, the 3d doubly occupied orbital is the lowest of a′ symmetry, which reduces repulsion through 4s3d hybridization, as pointed out by the value of the 4s natural population (about 0.7 electrons). However, in the $^5A''$ state, the doubly occupied orbital is a″ and the d−p mechanism by which it reduces repulsion is less efficient, the $^5A''$ state lying higher in energy than the $^5A'$ state.

The ground state of Fe^+−guanine and Fe^+−adenine is a $^4A'$ that arises from the $3d^7$ configuration of Fe^+. Although experimentally the $^6D(3d^64s^1)$ state of Fe^+ is the ground state, at the B3LYP level, the $^4F(3d^7)$ state becomes more favorable by 4.6 kcal/mol. This is a known error of DFT methods, which tend to stabilize d^{n+1} configurations with respect to sd^n ones.[35] This fact poses the question whether the quartet state is really the ground state of the complex or if this is an artifact of the method. However, if one considers that the error in the asymptote is carried over to the complex and we correct the computed values of the binding energies according to the

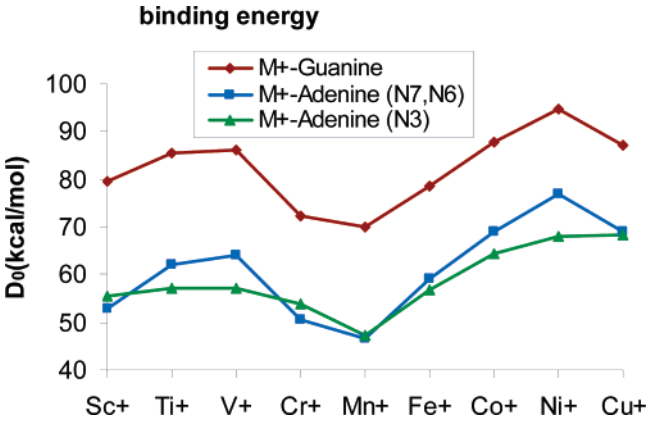

Figure 2. Variation of metal−nucleobase binding energy, in kcal/mol, along the row.

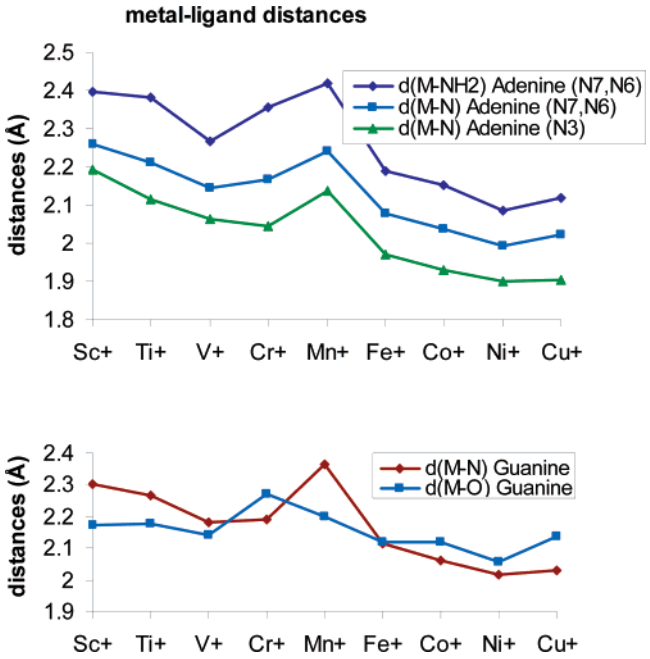

Figure 3. Variation of metal−nucleobase distances, in angstroms, along the row.

experimental values as explained in the methods section, the quartet remains the ground state in all cases (see Tables 1−3).

The $^4A''$ state arises from the same configuration of Fe^+ (d^7) and is almost degenerate with the $^4A'$ one. In both cases, repulsion with the ligand is reduced by 4s3d hybridization through mixing of both configuration asymptotes ($3d^7$ and $3d^64s^1$) because they are very close in energy. The sextet states ($^6A'$ and $^6A''$) are higher in energy than the quartets because the occupation of the 4s orbital enhances repulsion and 4s3d hybridization is no longer a viable mechanism to reduce repulsion, as shown by the natural population of Table 1.

The ground state of Co^+−guanine and Co^+−adenine is the $^3A'$ state, with the $^3A''$ state lying very close in energy (about 1 kcal/mol). Both states derive from the ground state configuration of Co^+ ($3d^8$). Again, 4s3d hybridization to reduce repulsion is evidenced by the natural populations. In the $^3A'$ state, the two open-shell orbitals are the highest energy ones of a′ symmetry, whereas in the $^3A''$, the unpaired electrons are in the $3d_{xz}(a')$ and $3d_{xy}(a'')$ orbitals.

The ground state of Ni^+−guanine and Ni^+−adenine is the $^2A'$ state derived from the Ni^+ $3d^9$ occupation with the hole in the $3d_{xz}(a')$ orbital to minimize repulsion. The natural population of the 4s orbital (see Table 1) indicates some 4s3d hybridization which further reduces the metal−ligand repulsion. The $^2A''$ excited state implies the double occupation of the most repulsive orbital of the metal, resulting in a much larger repulsion and thus a much smaller value of the binding energy as reflected in Table 1. The ground state of Cu^+−guanine and Cu^+−adenine is the closed-shell $^1A'$ state derived from the $3d^{10}$ ground state asymptote of Cu^+.

Trends. As mentioned, the bonding between M^+ and guanine and adenine is essentially electrostatic, the electronic ground state being mainly determined by metal−ligand repulsion; that is, the preferred metal d occupation is that in which electrons are allocated into the orbitals with smallest overlap with the ligand. Particularly unfavorable is the occupation of the d orbital that lies in the same plane of guanine or adenine and points toward the N and O lone pairs ($3d_{xz}$).

Figure 2 shows the variation of the binding energies along the row. First of all, it can be observed that guanine binding energies are larger than adenine ones. Nevertheless, variations along the row are similar, especially when comparing M^+−guanine (N7,O6) and M^+−adenine (N7,N6) bidentated systems. For these complexes, the binding energy increase from Sc^+ to V^+ as the size of the metal ion decreases and the $3d_{xz}$ orbital remains empty. However, for Cr^+ with a d^5 electronic configuration, this orbital becomes occupied, which leads to a strong repulsion with guanine or adenine that manifests in a decrease in the interaction energy. Mn^+ presents a slightly smaller interaction energy because the 4s orbital, with a larger spatial extent, is occupied, which leads to a larger repulsion. From Fe^+ to Ni^+, arising from the $3d^{n+1}$ configuration, the binding energy increases with increasing Z, paralleling the decrease in the ion size. For Cu^+, the binding energy decreases because the d orbital with largest overlap with the ligand becomes doubly occupied, increasing significantly the metal−ligand repulsion. For M^+−adenine N3 monodentate complexes, variations are similar but less pronounced because now the metal cation is interacting with only one basic site. On the other hand, the increase in Pauli repulsion upon occupation of the highest d orbital (from V^+ to Cr^+ and from Ni^+ tu Cu^+) is more important in the case of the bidentate systems than in the monodentate ones. As a consequence, differences between the bidentate (N7, N6) and the monodentate N3 coordinations decreases significantly for Cr^+ on the left side and Cu^+ on the right side of the row.

Similar arguments explain the variation in metal ligand distances along the row shown in Figure 3. That is, they tend to decrease from left to right, as the size of the metal ion decreases, although there are exceptions because of the different metal−ligand repulsion associated with different electronic configurations.

In M^+−guanine, the decrease in the M^+−N distances along the row is more pronounced than that of the M^+-O, in such a way that for right side metal ions, M^+−O > M^+−N, whereas the reverse is true for ions on the left side of the row. It is worth noting that the behavior of left side ions (Sc^+−V^+) is similar to that found for alkali cations, for which M^+−O < M^+−N. The M^+−N distances in M^+−adenine follow a similar variation along the row, the largest values obtained for Mn^+ systems because of the $4s^1d^5$ electronic configuration of the metal cation. On the other hand, it can be observed that the M^+−N distance corresponding to the amino group is larger than the M^+−(N7,N6) or M^+−N3 imino ones. Moreover, among the two latter distances, the M^+−N3 is about 0.1 Å shorter because of the monodentate character of the coordination, which,

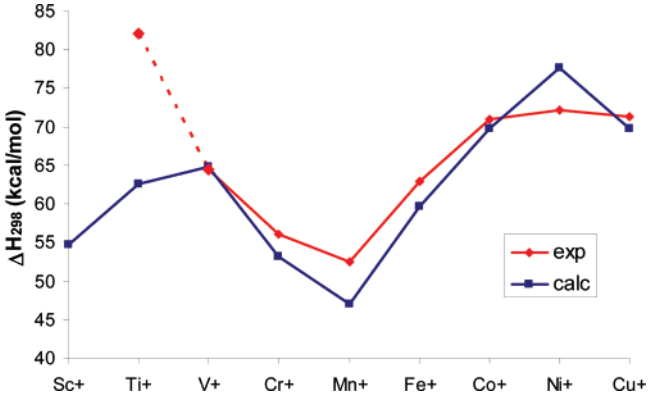

Figure 4. Cation affinities ΔH^0_{298} (in kcal/mol). The experimental value for Ti^+−adenine corresponds to an upper limit.

TABLE 4: Decomposition Analysis of the Binding Energy in kcal/mol (see text)

	Cu^+−guanine	Cu^+−adenine
prep	5.5	16.0
Pauli	77.9	91.3
elstat	−114.4	−117.3
orb	−60.9	−65.3
D_e	91.9	75.3

through sd hybridization, allows for a better reduction of metal−ligand repulsion.

Guanine vs Adenine. As found for alkali and alkaline-earth metal cations, the M^+−guanine interaction energy is larger than the M^+−adenine one by about 18−27 kcal/mol. Differences between the two interaction energies decrease along the row from 27 kcal/mol for Sc^+ to 18 kcal/mol for Cu^+ as the interaction with N becomes more favorable.

To analyze the main contributions to the binding energy of the considered systems, we have performed an analysis for the case of Cu^+−guanine and Cu^+−adenine using the partition scheme implemented in the ADF program.[45] Binding energies have been decomposed into the following terms

$$D_e = -(E_{prep} + E_{Pauli} + E_{elstat} + E_{orb})$$

E_{prep} is the preparation energy associated with the geometry distortion of guanine and adenine upon interaction with the metal cation. E_{Pauli} is associated with closed-shell repulsions between fragments. E_{elstat} is the electrostatic interaction energy arising from the interaction between both fragments, each fragment having the electron density that it would have in the absence of the other fragment. E_{orb} is the orbital interaction term that arises when the electron densities of both fragments are allowed to relax and accounts for charge transfer and polarization.

This decomposition analysis is shown in Table 4 and it can be observed that the difference in the binding energy of Cu^+−adenine and Cu^+−guanine mainly arises from the deformation energy of the purine, which is about 11 kcal/mol larger in adenine because of the rotation of NH_2 and loss of π resonance delocalization, and from the Pauli repulsion, which is about 13 kcal/mol larger in adenine. The difference in the Pauli term can be attributed to the larger repulsion of the occupied orbitals of Cu^+ with the lone pair of the NH_2 group (adenine) than with the lone pair of the oxygen (guanine) because of the different nature of both groups. The other terms (electrostatic and orbital interactions) are slightly favorable to adenine. Thus, considering all the interaction terms, the metal−purine interaction energy (Pauli repulsion + electrostatic + polarization + charge transfer) is about 6 kcal/mol larger in Guanine.

Comparison with Experimental Values. Figure 4 shows the variation in the experimental and calculated metal ion binding enthalpy of M^+−adenine along the row. Computed values have been determined using the B3LYP/BSII D_e and the B3LYP/BSI thermal corrections and correspond to the lowest state of the preferred coordination mode of each metal cations; that is, we have considered the N7, N6 bidentate coordination for all metal cations except for Sc^+ and Cr^+, for which the monodentate N3 binding is found to be more favorable. It can be observed that, except for the case of Ti^+, both experimental and calculated values are in quite good agreement, the average deviation being 3.2 kcal/mol. However, it should be mentioned that the reported experimental value for Ti^+−adenine corresponds to an upper limit of the binding enthalpy.

Conclusions

The interaction between guanine and adenine nucleobases and first-row transition metal monocations has been analyzed using the B3LYP density functional method. For guanine, coordination is found to be bidentate through the N7 and O6 sites. For adenine, we have explored two possible binding modes: the bidentate N7, N6 and the monodentate N3. For all metal cations, except Sc^+ and Cr^+, the bidentate coordination is the preferred one.

The nature of the bonding between guanine and adenine nucleobases and transition metal monocations (Sc^+−Cu^+) is found to be mainly electrostatic, the electronic ground state configuration being mainly determined by metal−ligand repulsion. That is, the ground electronic state derives from occupying those metal orbitals that show smaller overlap with the lone pair orbitals of the ligand, because this minimizes Pauli repulsion. Trends on metal ligand distances and binding energies are explained in terms of the size and electronic configuration of the metal ion. That is, metal−ligand distances decrease and interaction energies increase along the row, with the exceptions of $Cr^+(d^5)$, $Mn^+(4s^1d^5)$, and Cu^+ (d^{10}), for which metal−ligand repulsion increases significantly.

M^+−guanine interaction energies are systematically larger (about 18−27 kcal/mol) than those of M^+−adenine. Energy decomposition analysis for the Cu^+−guanine and Cu^+−adenine shows that differences mainly arise from the Pauli repulsion and deformation terms. That is, adenine undergoes heavier deformation in order to interact with the metal cation than guanine and Pauli electron−electron repulsion is also larger (more destabilizing) for M^+−adenine than for M^+−guanine, because of the different nature of the basic sites of the two nucleobases.

Finally, metal cation affinity values at this level of calculation are in very good agreement with the experimental data obtained by Rodgers et al.[8] for the adenine nucleobase. Computed M^+−guanine interaction energies are expected to behave in a similar manner and can be used to predict experimental values.

Acknowledgment. Financial support from MCYT and DURSI, through the CTQ2005-08797-C02-02/BQU and SGR2005-00244 projects, and the use of the Catalonia Supercomputer Centre (CESCA) are gratefully acknowledged.

References and Notes

(1) Martin, R. B. *Acc. Chem. Res.* **1985**, *18*, 32.
(2) Lippert, B. *Coord. Chem. Rev.* **2000**, *200*−*202*, 487.
(3) Bregadze, V. G. *Met. Ions Biol. Syst.* **1996**, *32*, 419.
(4) Eichorn, G. L.; Shin, Y. A. *J. Am. Chem. Soc.* **1968**, *90*.
(5) Rosenberg, B.; VanCamp, L.; Trosko, J. E.; Mansour, V. H. *Nature* **1969**, *222*, 385.

(6) Cerda, B. A.; Wesdemiotis, C. *J. Am. Chem. Soc.* **1996**, *118*, 11884.
(7) Rodgers, M. T.; Armentrout, P. B. *J. Am. Chem. Soc.* **2000**, *122*, 8548.
(8) Rodgers, M. T.; Armentrout, P. B. *J. Am. Chem. Soc.* **2002**, *124*, 2678.
(9) Song, B.; Zhao, J.; Griesser, R.; Meiser, C.; Sigel, H.; Lippert, B. *Chem.—Eur. J.* **1999**, *5*, 2374.
(10) Sun, J. L.; Liu, H. C.; Wang, H. M.; Han, K. L.; Yang, S. H. *Chem. Phys. Lett.* **2004**, *392*, 285.
(11) Anwander, E. H. S.; Probst, M. M.; Rode, B. M. *Inorg. Chim. Acta* **1987**, *137*, 203.
(12) Anwander, E. H. S.; Probst, M. M.; Rode, B. M. *Biopolymers* **1990**, *29*, 757.
(13) Burda, J. V.; Sponer, J.; Hobza, P. *J. Phys. Chem.* **1996**, *100*, 7250.
(14) Burda, J. V.; Sponer, J.; Leszczynski, J.; Hobza, P. *J. Phys. Chem. B* **1997**, *101*, 9670.
(15) Sponer, J.; Burda, J. V.; Sabat, M.; Leszczynski, J.; Hobza, P. *J. Phys. Chem. A* **1998**, *102*, 5951.
(16) Sponer, J.; Sabat, M.; Gorb, L.; Leszczynski, J.; Lippert, B.; Hobza, P. *J. Phys. Chem. B* **2000**, *104*, 7535.
(17) Russo, N.; Toscano, M.; Grand, A. *J. Phys. Chem. B* **2001**, *105*, 4735.
(18) Muñoz, J.; Sponer, J.; Hobza, P.; Orozco, M.; Luque, F. J. *J. Phys. Chem. B* **2001**, *105*, 6051.
(19) Russo, N.; Toscano, M.; Grand, A. *J. Am. Chem. Soc.* **2001**, *123*, 10272.
(20) Russo, N.; Sicilia, E.; Toscano, M.; Grand, A. *Int. J. Quantum Chem.* **2002**, *90*, 903.
(21) Russo, N.; Toscano, M.; Grand, A. *J. Mass. Spectrom.* **2003**, *38*, 265.
(22) Noguera, M.; Bertran, J.; Sodupe, M. *J. Phys. Chem. A* **2004**, *108*, 333.
(23) Sponer, J. E.; Sychrovsky, V.; Hobza, P.; Sponer, J. *Phys. Chem. Chem. Phys.* **2004**, *6*, 2772.
(24) Zhu, W.; Luo, X.; Puah, C. M.; Tan, X.; Shen, J.; Gu, J.; Chen, K.; Jiang, H. *J. Phys. Chem. A* **2004**, *108*, 4008.
(25) Kabelac, M.; Hobza, P. *J. Phys. Chem. B* **2006**, *110*, 14515.
(26) Lamsabhi, A. M.; Alcami, M.; Mo, O.; Yanez, M.; Tortajada, J. *Chemphyschem* **2004**, *5*, 1871.
(27) Lamsabhi, A. M.; Alcami, M.; Mo, O.; Yanez, M.; Tortajada, J. *J. Phys. Chem. A* **2006**, *110*, 1943.
(28) Marino, T.; Toscano, M.; Russo, N.; Grand, A. *Int. J. Quantum Chem.* **2004**, *98*, 347.
(29) Mazzuca, D.; Russo, N.; Toscano, M.; Grand, A. *J. Phys. Chem. B* **2006**, *110*, 8815.
(30) Russo, N.; Toscano, M.; Grand, A. *J. Phys. Chem. A* **2003**, *107*, 11533.
(31) Schreiber, M.; Gonzalez, L. *Chem. Phys. Lett.* **2007**, *435*, 136.
(32) Becke, A. D. *J. Chem. Phys.* **1993**, *98*, 5648.
(33) Becke, A. D. *J. Chem. Phys.* **1993**, *98*, 1372.
(34) Lee, C.; Yang, W.; Parr, R. G. *Phys. Rev. B* **1988**, *37*, 785.
(35) Bauschlicher, C. W.; Ricca, A.; Partridge, H.; Langhoff, S. R. *Recent Advances in Density Functional Theory, Part II*; World Scientific Publishing Co.: Singapore, 1997.
(36) Blomberg, M. R. A.; Siegbahn, P. E. M.; Svensson, M. *J. Chem. Phys.* **1996**, *104*, 9546.
(37) Holthausen, M. C.; Mohr, M.; Koch, W. *Chem. Phys. Lett.* **1995**, *240*, 245.
(38) Koch, W.; Holthausen, M. C. *A Chemists's Guide to Density Functional Theory*, 2nd ed.; Wiley-VCH Verlag: Weinheim, Germany, 2001.
(39) Ricca, A.; Bauschlicher, C. W. *Chem. Phys. Lett.* **1995**, *245*, 150.
(40) Wachters, A. J. *J. Chem. Phys.* **1970**, *52*, 1033.
(41) McQuarrie, D. *Statistical Mechanics*; Harper and Row: New York, 1986.
(42) Weinhold, F.; Carpenter, J. E. *The Structure of Small Molecules and Ions*; Plenum: New York, 1988.
(43) Frisch, M. J.; Trucks, G. W.; Schlegel, H. B.; Scuseria, G. E.; Robb, M. A.; Cheeseman, J. R.; Montgomery, J. A., Jr.; Vreven, T.; Kudin, K. N.; Burant, J. C.; Millam, J. M.; Iyengar, S. S.; Tomasi, J.; Barone, V.; Mennucci, B.; Cossi, M.; Scalmani, G.; Rega, N.; Petersson, G. A.; Nakatsuji, H.; Hada, M.; Ehara, M.; Toyota, K.; Fukuda, R.; Hasegawa, J.; Ishida, M.; Nakajima, T.; Honda, Y.; Kitao, O.; Nakai, H.; Klene, M.; Li, X.; Knox, J. E.; Hratchian, H. P.; Cross, J. B.; Adamo, C.; Jaramillo, J.; Gomperts, R.; Stratmann, R. E.; Yazyev, O.; Austin, A. J.; Cammi, R.; Pomelli, C.; Ochterski, J. W.; Ayala, P. Y.; Morokuma, K.; Voth, G. A.; Salvador, P.; Dannenberg, J. J.; Zakrzewski, V. G.; Dapprich, S.; Daniels, A. D.; Strain, M. C.; Farkas, O.; Malick, D. K.; Rabuck, A. D.; Raghavachari, K.; Foresman, J. B.; Ortiz, J. V.; Cui, Q.; Baboul, A. G.; S. Clifford; Cioslowski, J.; Stefanov, B. B.; Liu, G.; Liashenko, A.; Piskorz, P.; Komaromi, I.; Martin, R. L.; Fox, D. J.; Keith, T.; Al-Laham, M. A.; Peng, C. Y.; Nanayakkara, A.; Challacombe, M.; Gill, P. M. W.; Johnson, B.; Chen, W.; Wong, M. W.; Gonzalez, C.; Pople, J. A. *Gaussian 03*, revision B.04; Gaussian Inc.: Pittsburgh, PA, 2003.
(44) *ADF2005.01*; SCM, Theoretical Chemistry, Vrije Universitat: Amsterdam; http://www.scm.com.
(45) te Velde, G.; Bickelhaupt, F. M.; Baerends, E. J.; Fonseca-Guerra, C.; van Gisbergen, S. J. A.; Snijders, J. G.; Ziegler, T. *J. Comput. Chem.* **2001**, *22*, 931.
(46) Bickelhaupt, F. M.; Baerends, E. J. *Rev. Comput. Chem.* **2000**, *15*, 1.
(47) Frenking, G.; Froehlich, N. *Chem. Rev.* **2000**, *100*, 717.
(48) Leszczynski, J. *Int. J. Quantum Chem. Quantum, Biol. Symp.* **1992**, *19*, 43.
(49) Sponer, J.; Hobza, P. *J. Phys. Chem.* **1994**, *98*, 3161.